In Biology-Inspired Maneuvering Hydrodynamics for AUV Application
Frank E. Fish, Editor
Working copy, Version 7/17/03, Do Not Cite

Kinematics and Performance of Maneuvering Control Surfaces in Teleost Fishes

Jeffrey A. Walker

I. Introduction

Teleost fishes present a wide diversity of both maneuvering behaviors and hydrodynamic mechanisms to control maneuvering. Maneuvering behaviors include small yaw and pitch turns that either correct perturbations to some desired heading or reorient fish in a new heading, large yaw and pitch turns that are used to reverse direction, rapid yaw turns used for escape from a threatening stimulus, rapid accelerations for escape or the pursuit of prey, braking, reversing and hovering in still water or a bidirectional surge. The ability to exploit resources in structurally complex and high-energy habitats such as wave swept rocky shores and coral reefs using a diverse repertoire of maneuvering behaviors suggests that fishes are a good model for transferring biological information to the design and control of autonomous undersea vehicles (AUVs). While the entire body and fin surface of fishes function in maneuvering control, the combination of fin and body motions necessary to actuate a maneuver differ both within individuals among behaviors and within behaviors among individuals and species. A qualitative comparison of swimming behavior among a diverse array of fishes suggests two general principles. First, while axial (body) undulations are used by most fishes for steady swimming at typical cruising speeds, maneuvers are commonly controlled by fin motions with or without axial bending. Second, the tremendous variation in the combination of fin shapes and motions suggest that no single phenotype is optimal for the complete suite of maneuvering behaviors. The goal of this paper, then, is not to suggest the best species for an AUV blueprint because the design of any one species reflects both the distinct signature of its history and a mind-boggling array of trade-offs due to competing demands on functional systems. Instead, the goal of this paper is to review the kinematic control mechanisms used for maneuvering, compare the performance consequences of this variation, and use general principles distilled from these studies to suggest biology-inspired technologies for AUV design that best match the desired function.

This work was supported in part by the U.S. Office of Naval Research under Grant N00014-01-1-0506.

J. A. Walker is with the Department of Biology, University of Southern Maine, 96 Falmouth St., Portland ME 04103 USA (207-228—8166; fax: 207-228-8116; e-mail: walker@usm.maine.edu

II. Control Surface Motions

A. Body and Caudal Fin (BCF) Motion

Axial deformations are used for yaw turns in nearly all fishes, and braking [1, 2], and reversing [3] in some fishes. Following [4, 5], I refer to axial bending powered maneuvers as body and caudal fin (BCF) maneuvering. The surfaces of median and caudal fins in BCF maneuvering are generally treated as stiff extensions of the body and without independent actuation mechanisms. Deformations of the caudal fin *sensu stricto* will not be reviewed here but have been discussed in [6]. Median fin motions by muscles that directly actuate the median fin bony rays are described below.

The BCF control of routine turns has not been systematically investigated but qualitative and quantitative descriptions of axial bending and turning behavior have been described [7-9]. BCF motions that generate large accelerations and rapid rotations have been intensely investigated. A brief description of the kinematics is given here but the reader is referred to the thorough review in [10]. There are two general kinematic modes of BCF powered accelerations: C-starts, which are generally associated with startle or escape responses, and S-starts, which are generally associated with predation strikes. A C-start is typically divided into three stages [7]. In stage I, the axial muscles along all or most of one side contract strongly, which bends the fish into a C-shape. This initial bending might result from either simultaneous muscle contraction along the axis or a very rapid moving wave. In stage II, a large amplitude, traveling wave of contralateral muscle contraction rapidly passes from anterior to posterior. Stage III is variable, but can include braking, gliding to a stop, small to moderate axial undulations that maintain swimming speed, or moderate to large amplitude axial undulations that continue to accelerate the fish. S-start kinematics differ mainly in the S-shape that occurs at the end of stage 1.

B. Median and Paired Fin (MPF) Motions

Fin anatomy is highly relevant to fin motions and is reviewed in the chapter by Lauder. The fins of actinopterygian (bony ray) fishes are supported and controlled by multiple, bony rods, or fin rays. Four muscles insert onto the base of each ray, potentially allowing a full two degrees of freedom at each fin ray joint. Qualitative investigations of fin motions suggest that fishes have large control over the patterns of fin muscle activation and, ultimately, fin deformations (hence reducing the influence of external fluid dynamic and internal elastic stresses). Consequently, fin motions of fishes can be much more

complex than the typical heaving and pitching motions of rigid wings or even chordwise flexible wings controlled at a single support axis. Not surprisingly, the kinematics of the fin motions varies tremendously within and among individuals, populations, and species.

1) Median Fin Deformations: Median fins vary greatly in both shape and deformations. Much of the recent focus on median fins has been on the kinematic, fluid dynamic and performance differences between long-based, low aspect ratio (AR), undulatory median fins and long-based, high AR, flapping median fins [11-14]. But median fin shape and motion are highly variable. The "soft," posterior portion of the dorsal fin in the bluegill sunfish oscillates independently of the body and contributes to the thrust balance during steady swimming [15]. The short-based, fan (or pectoral fin) shaped median fins of boxfishes, pufferfishes and burrfishes contribute to the thrust balance during steady swimming [16-18] and are active during yaw-turning maneuvers [19].

More relevant to this review are the dorsal and anal fin motions that contribute to maneuvering. Following a pectoral fin actuated yaw rotation of small magnitude (about 25°) while swimming in a slow current (0.5 L/s), the soft (posterior) portion of the median fin of the bluegill sunfish rapidly abducts in a direction opposite that of the turn [15]. The median fin motion generates a force directed medially and anteriorly, generating a torque of the opposite sign to that generated by the pectoral fins. This torque would have the effect of returning the heading back to a direction parallel with the flow.

Breder [20] suggested that the median fins of tetraodontids (pufferfishes) could generate yaw-rotational torques by limiting oscillation to the side of the mid-sagittal plane in which the fish is turning. It would seem that limiting the motion to one side of the mid-sagittal plane is not necessary if the fin can create unbalanced forces when oscillating to one side versus the other. Because of their very narrow base and distally expanded, paddle shaped surface, the median fins of pufferfishes, boxfishes, and burrfishes should be able to translate broadside during one stroke and feathered during the opposite stroke. The illustration of dorsal and anal fin motion during yaw turning in the boxfish *Tetrasomus gibbosus* suggests these fins neither feather during one stroke nor limit their motion to one side of the midsagittal plane [19]. The illustration of the *T. gibbosus* dorsal fin does show that the posterior region of the fin base can be actively rotated relative to the anterior region by about 40°.

2) Pectoral Fin Deformations. Deformations of the pectoral fins during steady swimming have been described in great detail and are reviewed here in order to facilitate the discussion of the motions during maneuvering.

a) Pectoral fin deformations during steady swimming. Most of the focus on variation in pectoral fin motion has been on hydrodynamic, performance, and ecological differences between "rowing" along a horizontal stroke plane and "flapping" along a vertical stroke plane [20-27] during steady swimming. Both rowing and flapping include heaving (root oscillation of the fin back and forth along the stroke plane) and pitching (rotation of the fin around a spanwise axis) motions (Fig. 1). The stroke plane is constrained by the geometry of the fin-ray joint within the fibrocartilage pad of the shoulder plate, the orientation of the fibrocartilage pad, and by the mobility of the joints within the shoulder plate (four bony radials and the fibrocartilage pad) (see chapter by Lauder). The fin ray joints allow a large major axis of motion (that occurring along the stroke plane) and a smaller minor axis of motion (normal to the stroke plane). The fibrocartilage pad is curved [28], which might create variation in the major axis of mobility among the rays. The surface swept out by the leading edge of a pectoral fin is not a plane but a slightly curved surface that is inclined more vertically during fin abduction and more horizontally during fin adduction [18, 29-34]. The difference between the abduction stroke plane angle and adduction stroke plane angle is greater in fishes that present more of a rowing stroke [34]. The orientation of the abduction and adduction stroke planes can also vary among strokes, typically as a function of swimming speed [18, 34]. Fishes at the rowing-flapping extremes, such as the threespine stickleback, a stereotypical rower, and the bird wrasse, a stereotypical flapper, present little variation in stroke plane angle with speed [24]. By contrast, fishes that are more intermediate between rowing and flapping may either decrease [18] or increase [34] the steepness of the stroke plane as speed increases (although the stroke plane angles never reach the extremes of the stickleback and the bird wrasse). The anatomical mechanism allowing this limited variation in stroke plane angle within individuals has not been investigated but could include both rotation of the fin root (the fibrocartilage pad) and some component of fin ray motion along the minor axis of the fin ray joint. No substantial (>5°) fin root rotation was noticed in threespine sticklebacks or the wrasses (Walker, unpublished observations) but large root rotations (up to 30°) have been illustrated for boxfish [19] and trout [35]. It should be noted that the mean stroke plane angle (the mean of the abduction and adduction stroke plane angles) is not perpendicular to the major axis of the fin root but there is a correlation between the orientation of the fin root and this mean angle among species [27].

Reorientation of the fin root at the shoulder plate is one of two mechanisms for pitching the fin. Rotation of the fin root rotates the fin uniformly along the span and is, therefore, functionally similar to the pitching mechanism found in insect wings and motorized, oscillating fins such as those in a robotic fruit fly [36] and bass [37, 38]. The degree to which fish can rotate the fin root has not been investigated and probably varies among species as a function of shoulder plate mobility [39, 40]. Regardless of the amount of rotation at the fin root, the primary mechanism that fish exploit to pitch the fin is by controlling the phase variation between leading and trailing fin rays (as described for fin undulation above). The larger the phase lag between leading and trailing edge (up to 180°) the larger the pitch amplitude. Unlike rotation of the fin root, however, this mechanism does not rotate the fin as a rigid plate but dynamically twists the fin along its span. The twisting generates a spanwise gradient of chord pitch amplitudes; the pitch amplitude is necessarily zero at the fin root (i.e. all pitching at the root must come from reorientation of the fin root) and increases to its maximum, which should occur not at the fin tip but at the spanwise location containing the tip of the trailing edge ray. Because of the separate

tendinous insertion of the abductor and adductor muscles on each ray, actinopterygian fishes should have large, active control of the deformations that generate this spanwise gradient of pitch.

The pitch, or orientation, of a chordwise segment relative to a horizontal (frontal) plane at time *t* and spanwise position *r* is $\theta_m(t, r)$. The change in θ_m during a stroke cycle for a distal chord element is not a simple harmonic function for either an extreme rower (threespine stickleback) or an extreme flapper (bird wrasse) (Fig. 1). For a rowing fin, we expect this from the simple principle that mean thrust should be maximized by minimizing θ_m (i.e. $\theta_m = 0°$) throughout the recovery stroke and maximizing θ_m (i.e. $\theta_m = 90°$) throughout the power stroke. Indeed, we find this general pattern in the stickleback (Fig. 1). In the stickleback, θ_m rapidly falls from 90° to 10° at the beginning of the recovery stroke, gradually drops to –20° at the end of the recovery stroke, and rapidly climbs to and is maintained at 85° at the beginning of the power stroke. The negative θ_m for the distal element during the recovery stroke reflects a constraint of using a phase lag between leading and trailing edge to generate fin pitch. The fin root of the stickleback is oriented about 70° from the horizontal. Were the fin root able to rotate to 0°, the entire fin could optimally feather (i.e. $\theta_m = 0°$) during the recovery stroke. By twisting the fin, optimum feathering during the recovery stroke can only occur at a single spanwise position; θ_m will be greater than zero proximal to this position and less than zero distal to this position. The spanwise position of this optimum, which will ultimately determine the abduction pitch amplitude at the fin tip, is that point which minimizes the integral of $cU^2|\theta_m|$ along the span, where *c* is the fin chord, *U* is the tangential velocity of the fin element and the brackets represent the absolute value.

In the bird wrasse, θ_m rapidly drops to about –10° during the downstroke and maintains this level until the beginning of the upstroke. About halfway through the upstroke, θ_m reaches its peak of 60°. As predicted by a simple rowing-flapping model [22, 24], the upstroke θ_m is substantially less than the power stroke θ_m of the bird wrasse. Nevertheless, an asymmetry between downstroke and upstroke θ_m differs from the symmetric angles predicted by an idealized, neutrally buoyant flapping fin (that is, the absolute value of the positive and negative pitch amplitudes should be the same). Indeed, this difference from the idealized model reflects the negative buoyancy of the bird wrasse and the necessity of generating a net upward force during the stroke cycle. As in birds and insects, the stroke plane angle of the bird wrasse is tilted back to create an upward component to the mean force over a stroke cycle. The stroke plane angle of the bird wrasse is about 20° from the vertical [33] while the θ_m peaks are symmetric about a midpoint of 25° (Fig. 1).

A spanwise twist mechanism of pitch control should be more effective than a root-rotation mechanism of pitch control for flapping propulsion if there is a strong spanwise gradient in the angle of the incident flow. This might occur, for example, at moderate advance ratios, where the flapping component of the incident flow dominates at the tip while the translational component of the incident flow dominates at the fin base. Given the change in the indent flow angle down the span, the spanwise twist allows the fin pitch to match the optimal pitch, which also changes (increases) down the span. Indeed, spanwise twisting is a common feature of the flapping stroke among many aquatic animals other than fishes, including pterapod gastropods, finned cephalopods, and sea turtles (see references in [23, 41]. In contrast, at low advance ratios, a root-pitching fin may be more effective because large incident flows at high angles (and consequently, forces) would occur along the entire span during the rotational phases of the stroke cycle. This stroke geometry would allow the animal to take advantage of the large rotational forces occurring during rotational phases. Importantly, differences in the timing and duration of the rotational phases between fins have been shown to be important for insect maneuverability [42]. Even fishes without a root-pitching fin could exploit this rotational mechanism if the trailing edge ray is short relative to the leading edge ray (a geometry that would allow the fin distal to the trailing edge tip to rotate semi-rigidly). For example, during steady swimming in the bird wrasse, the distal fin chord does not pitch with a substantially larger amplitude than the proximal fin chord (located at the spanwise position of the tip of the trailing edge ray), indicating that much of the fin is rotating semi-rigidly (see Fig. 13 in [33]).

A root-pitch mechanism is more effective for rowing because this allows perfect feathering along the span during the recovery stroke and perfect broadside orientation during the power stroke [23]. In many animals with spanwise segmented limbs that have mobile intersegmental joints, including some mammals [43], freshwater turtles [44], and large water beetles [45, 46], only the distal segment is expanded into a propulsive paddle. “Root” pitching rotation of the stiff (untwisted) distal segment occurs by rotation at one or more intersegmental joints.

Root pitching is only effective when the joint allowing pitching rotation is distal to the joint allowing limb heaving (that is, the pitching joint oscillates with the limb). This geometry occurs in beetles and tetrapods but not actinopterygian fishes. Root rotation in fishes would require that the fin rays oscillate along the minor axis of the fin ray joint during the recovery stroke and along the major axis of the joint during the power stroke. The elliptical geometry of the fin ray joints do not allow large motions along the minor axis. Hence, for rotation to be effective in fishes, the fin ray joints would have to have a ball and socket geometry, which would most likely compromise the stability of the joint when highly loaded.

While the root-pitching mechanism of pitch control is optimal for the translation phases of the stroke cycle, the spanwise twisting mechanism may actually be more effective during the stroke transition phases. Root-pitching will generate large vertical in addition to horizontal forces [36, 47, 48]. At the beginning of the transition to the recovery stroke, when the fin initiates movement away from the body, counterclockwise rotation of the fin about the trailing edge will generate an upward force in addition to a horizontal force with a large medial and small drag component. Rapid counterclockwise rotation about the leading edge would generate a downward force in addition to a horizontal force

with a large lateral and small thrust component. But in this latter example, the presence of the body would limit the rate of counterclockwise rotation (because the fin cannot rotate into the body) and, with limited rotational speed, the net force would be upward, medial and backwards. At the beginning of the transition to the power stroke, clockwise rotation about the leading edge will generate an upward force and a horizontal force with a large drag and small medial component. In contrast, rapid clockwise rotation about the trailing edge will generate a downward force and a horizontal force with moderate thrust and small lateral components. If a fish is near neutral-buoyancy, these vertical force components represent wasted energy.

The spanwise twisting mechanism of pitch control in the stickleback enables this fish to avoid the large vertical forces during the rotational phases (Fig. 2). Immediately prior to the recovery stroke in the stickleback, the fin rotates counterclockwise along the body. The first part of the recovery stroke is characterized by the fin rays peeling off the body starting with the leading edge ray and proceeding, ray by ray, to the trailing edge ray. As the leading edge rays peel off the body, the trailing rays continue to rotate counterclockwise along the body. The point marked by the red arrow in Fig 2 illustrates the break point along the distal edge separating the hydrodynamically active leading edge region from the inactive trailing region. The trailing edge ray peels off the body about the time it reaches the same dorsoventral position as the leading edge ray. The second part of the recovery stroke is characterized by the fin translating anteriorly with the plane of the fan pitched slightly ventrally (Fig. 2).

The power stroke of the stickleback begins with a rapid dorsocaudal translation of the leading edge ray. The dorsal translation of the leading edge causes a clockwise rotation of the anterior fin surface into a broadside orientation (Fig. 2). A wave of fin ray rotation passes posteriorly as the leading edge rays translate posteriorly. During the posterior translation of the leading edge surface, the trailing rays stopped translating anteriorly but may move slightly ventrally. The red arrow in Fig.2 illustrates the break point on the distal edge marking the leading edge region, which is rapidly translating posteriorly, from the trailing edge region, which has largely stopped translating. During this time, the fin is sharply cuved at this break point. It is important to note that the fin does not rigidly rotate into a broadside orientation but instead resembles the peeling of a carpet off a floor by pulling one end back and up. Following rotation, all fin rays simultaneously translated back toward the body (Fig. 2). A similar pattern of fin ray peeling during the transitions between recovery and power strokes was described for the boxfish, *Ostracion meleagris* [18].

In addition to the root-pitching and spanwise twisting mechanisms of pitch control during the recovery and power strokes, many animals present a third mechanism for feathering: passive appendage feathering resulting from fluid dynamic loading on the paddle or paddle elements. In small water beetles and zooplankton, the paddle is not a solid surface but instead a central shaft supporting numerous swimming hairs [46, 49]. The joint between the hair and the shaft allows fluid dynamic stresses to collapse the hairs against the shaft during the recovery stroke but extend the hairs away from the shaft during the power stroke. No rotation is necessary and the transition between power and recovery strokes is very rapid. This mechanism is scale dependent; at low Reynolds numbers, the hairy shaft effectively acts like a solid paddle because of the relatively large boundary layer surrounding each hair [50]. In larger animals with webbed feet, such as ducks and frogs, passive feathering results from fluid-dynamic powered flexion at the ankle joint.

b) Pectoral fin deformations during maneuvering behaviors. Despite the many recent papers on fin control of steady swimming, our understanding of fin control of maneuvering has not progressed much beyond [20]. This lack of progress may reflect the much more diverse array of motions occurring among maneuvering pectoral fins. What is especially lacking are data on the kinematic differences occurring with different levels of performance.

All fish apparently oscillate the pectoral fins during hovering in still water. Breder [20] rejected equilibrium-maintenance and fresh-water-maintenance explanations of pectoral fin movement in favor of the suggestion that pectoral fin motions balance the thrust generated by ventilating gills. Blake [51] investigated the effects of distance above the floor on the frequency and amplitude of undulatory motions of the hovering pectoral fins of the mandarin fish *Synchropus picturatus*, but there is not enough of a qualitative or quantitative description of fin deformations to understand how the fore-aft forces cancel and how the fin generates a net upward force that balances the weight of the body. The rainbow trout, *Oncorhyncus mykiss*, oscillates its ventrally positioned pectoral fins at high attack angles in a largely sagittal plane [35] (Fig. 3). On the abduction (protraction) stroke, drag generated on the fin due to a large flow separation and the creation of an attached vortex on the downstream surface contributes to drag at the center of mass. Because the fins alternate out of phase, the opposite-side adducting (retracting) fin should generate a similar separation, vortex formation, and resulting drag, which, acting as thrust at the center of mass, balances the fore-aft forces. An attached vortex on the downstream surface of the adducting fin is not visible in the photo.

During hovering in the threespine stickleback, *Gasterosteus aculeatus*, the pectoral fin rays oscillate anteroposteriorly with a large phase lag between leading and trailing edge (personal observation). A wave is passed from leading (dorsal) to trailing (ventral) edge, creating a large positive angle of attack (around 45°) relative to the horizontal in both abduction (foreward) and adduction (backward) strokes. The large angle of attack and the ventrally propagating wave generate an upward force that balances the negative buoyancy of the fish while the symmetry in the angle of attack between abduction and adduction strokes cancels fore-aft forces.

Breder [20] suggested that pectoral fins generate turning moments and centripetal forces by one of two mechanisms. First, the inside fin (that on the inside of the turn) is held against the body while the outside fin (that on the outside of the turn) oscillates as in steady swimming; the thrust generated by the fin contributes to the rotational torque on the center of mass. Second, the outside fin is held against the

body while the inside fin is extended laterally; the drag generated by the fin contributes to the rotational torque on the center of mass.

Blake [19] illustrated the adduction (or powerstroke) of the outside pectoral fin in a yaw turn of the boxfish *Tetrasomus gibbosus*. The illustration shows the fin adducting toward the body with the geometric angle of attack remaining relatively constant around a value of 25°. Simultaneously, a moderate-amplitude wave is passed from the leading (dorsal) to trailing (ventral) edge. According to [19], the inside fin is either held against the body or oscillates with the reverse motions of the outside fin.

Some observations on the deformations of the pectoral fins during yaw turning in the boxfish, *Ostracion meleagris* can add to this description. In the 195° turn illustrated in Fig. 3 of [52], the outside fin makes five full fin beat cycles while the inside fin makes two full cycles. The outside fin strokes are similar to the steady swimming stroke described for the stickleback except that each stroke is of large amplitude (the leading edge abducts to about 165° from a posteriorly oriented vector). The drag created by the power stroke of the fin contributes to the rotational torque about the center of mass. For the first 90° of the turn, the inside fins remains extended in a roughly feathered orientation with the leading edge abducted about 116° and the trailing edge about 25° (Fig. 4). From this abducted, feathered position, the inside fin stiffly supinates about an axis near the leading edge, which should produce a large drag (an upward) component on the fin that adds to the rotational torque. During this rotation phase, the fin rays abduct; at the end of the rotation and abduction, the leading edge is 158° abducted while the trailing edge is 190° abducted (the sharply angled lateral wall of the body anterior to the pectoral fin allows this hyperabducted motion although it is not clear if muscle shortening or inertial forces cause the hyperabduction) (Fig. 4). Following the supination and abduction, the inside fin adducts and pronates about an axis close to the leading edge. The pronation is not a stiff-plate rotation (as in the supination) but is executed as a wave (similar to the rotation phase described for the stickleback pectoral fin), which presumably generates less drag on the fin (which would subtract from the rotational torque). At the end of the pronation phase, the inside fin has returned to a feathered orientation with the leading edge at 150° and the trailing edge at 33°. The inside fin makes a second beat that starts with a stiff supination about the 1/4 chord axis. At the end of this supination the leading edge has adducted to 95° while the trailing edge is at 130°. This second supination is followed by a stiff pronation into a feathered orientation. The stiff pronation should generate a downward and forward force that both slows rotation and increases acceleration away from the turn. Finally, it should be noted that in some turns, the inside fin executes a feathered adduction stroke led by the leading edge ray (requiring a large spanwise twist).

The bluegill sunfish, *Lepomis macrochirus*, uses both inside and outside pectoral fins to generate small turning moments at low swimming speeds [53]. As shown in Fig. 5, peak rotational velocity occurs when the outside fin rapidly adducts from an initially strongly abducted position while the ipsiliateral fin slowly adducts from an initially weakly abducted position. Both the inertial force at the beginning and the circulatory force at the middle of the outside fin adduction stroke should contribute to the rotational torque. During its initial abducted position, it may generate drag that contributes to the torque. The large posteriorly directed jet that develops by the end of the stroke however suggests that the fin, at least during adduction, creates a torque of opposite sign, which may serve to brake the rotation.

III. Performance

Maneuvering behaviors are composed of one or more measurable, whole-animal performances, such as braking acceleration, turning radius, turning rate, etc. Whole-animal performance, in turn, is a function of multiple, interacting physiological systems influencing the ability of the fish to deform multiple control surfaces, of fluid dynamic and inertial properties of the body and control surfaces, and of fluid dynamic interactions among control surfaces and between control surfaces and the body. Experimental and computational investigation of control-surface performance within isolated and interacting model fins is reviewed in more detail by Triantafyllou (Chapter xxx) and Mittal (Chapter xxx) while aspects of whole animal performance from a quantitative wake visualization perspective is reviewed in Lauder (Chapter xxx). In this section, I will concentrate on measures of whole-animal performance components and how these are related to control-surface performance. The review is limited to yaw turning performance, because there are too few data from other types of maneuvering for comparison. The only comprehensive study of a wide variety of maneuvering performances is [5].

Yaw turns are actuated by creating a net turning moment, or torque, about a dorsoventral axis that runs through the center of mass. Turns are powered by some combination of passive and active control surfaces. A passive control surface (a fin or region of the body) held at an angle to the local flow, creates an asymmetric pressure distribution over the surface and a turning moment about the axis of rotation. The energy for passive (or trimmed) turn arises from the kinetic energy of the moving fish (or moving water if the control surface is held in a current). An actively moved control surface generates both circulatory (drag and lift) and inertial forces that, in turn, contribute to the net turning moment about the axis of rotation. The energy for an active (or powered) turn arises from the work of the muscles actuating the control surface.

A. Yaw Turning Performance Measures

For fishes, as with AUVs, there is no single best measure of turning performance. High linear and rotational velocities and accelerations should augment evasive maneuvers from predators. The ability to rapidly and precisely reposition one's orientation over a broad range of angular displacements should facilitate inspection behavior (scanning a territory, searching for prey) and correct for small perturbations to the heading. Low turning radius turns should increase the ability of fishes to exploit resources in structurally complex environments such as submerged vegetation or coral reefs. Turning with high efficiency saves energy that could be

allocated to other functions or behaviors. None of these variables have been measured in any single study. Some, such as the ability to precisely reposition one's orientation, are poorly defined, do not have an easily measured performance, and have not been measured. Others, such as rotational accelerations, are easily defined and measured, but have not been reported in any study. Still others, such as turning with high efficiency has been measured in behaviors (fast-start escape responses) in which efficiency is unlikely to be the performance variable that the deforming body is optimizing.

Two types of turning performance measures have been explored: Translational variables, which are some function of the linear displacement of the center of mass, and rotational variables, which are some function of the angular displacement of the anterior body (the line segment in the median sagittal plane connecting the anterior tip of the snout and the stretched-straight center of mass). Rotational variables have been estimated from center of mass displacement but in boxfish, at least, the duration of body rotation can be much longer than the duration of body translation around a turning arc [52].

Translational variables that have been reported include maximum linear velocity and acceleration, minimum coefficient of normal acceleration, and minimum turning radius. The coefficient of normal acceleration [54] is the gravity-standardized acceleration normal to the turning path. While the turning radius is always reported as a single number, the radius of curvature along a turning path is generally not constant (Fig. 6). Walker [52] used numerical differentiation to estimate instantaneous radius of curvature along the turning path of boxfish and reported the minimum radius along the path as the measure of maximum performance. At least for boxfish, this is somewhat unsatisfying as the minimum radius does not capture the shape of the turning curve. More recently, Walker (unpublished data) computed the major and minor axes of the turning path and used these as additional performance variables (Fig. 6).

Peak rotational acceleration, $\dot{\omega}_{max}$, during a turn would be a useful variable for comparison, since it is most directly related to control surface performance (net maximum torque generated by the control surfaces), but $\dot{\omega}_{max}$ for any fish has yet to be reported. Peak rotational velocity, ω_{max}, has been reported and is closely related to control surface performance if the duration of the turn is greater than that necessary to achieve $\dot{\omega}_{max}$. More typically, the average rotational velocity over a turn, ω_{avg},, is reported. ω_{avg} is a function of the duration of the turn in addition to the torque generated by the control surfaces and the inertial and drag resistance of the body. Variation in duration will reflect both morphophysiological differences, including differences in muscle contractile durations and inertial resistance to body deformations [55, 56], and the total angular displacement of the turn, $\Delta\theta$. Indeed, Domenici and Blake [57] have shown a negative correlation between $\Delta\theta$ and ω_{avg} .

Three yaw-turn designs that are relevant to AUV and fish maneuvering are compared. Pectoral fin (PF) turns are actuated by one or both pectoral fins. The outside fin employs its optimal thrust-generating motion (in general, this should be a rowing motion) while the inside fin employs is optimum drag-generating motion (in general, this could be braking with an extended fin or "reverse" rowing). The fins generate a combined moment that rotates the heading of the fish toward the inside. Caudal fin (CF) powered turns are actuated by the caudal fin swinging about a base located somewhere along the caudal peduncle. Inertial and circulatory forces on the fin will generate large yaw torques that will rotate the fish (note that the sign of the torque occurring at the end of the stroke will be opposite to the that occurring halfway through the stroke and at the beginning of the stroke). Caudal body (CB) powered turns are similar to CF turns but a flexible body swings the caudal body (which may include the median fins if these are posteriorly positioned) and caudal fin about the center of mass (in general, this motion is not stiff but is generated by a wave of bending that passes caudally).

B. Yaw Turning Performance Variation

1) Turning Radius. The most common measure of turning maneuverability is the turning radius, R, which decreases with increased performance, or its reciprocal, turning curvature, κ. R is a function of the kinetic energy of the fish and the centripetal force:

$$R = \frac{mV^2}{F_c} \tag{1}$$

where m is the virtual mass (the sum of the fish and added mass), V is the tangential velocity of the center of mass, and F_c is the centripetal force, which is the sum of the components of the circulatory and inertial forces on each control surface that are normal to the heading of the fish. If we substitute into equation (1) the circulatory centripetal force,

$$F_{c,r} = \tfrac{1}{2}\rho S U^2 C_N \tag{2}$$

where ρ is the density of the water, S is the area of the control surface, U is the resultant velocity of the control surface, U is the resultant velocity of the control surface at the center of the force distribution, and C_N is the coefficient of the component of net force normal to the heading of the fish, then

$$R \quad (m/S)(V^2/U^2) \tag{3}$$

Two useful conclusions can be drawn from equation (3). First, if the body or gliding wings or fins are generating F_c, then $U \propto V$ and R will be independent of speed as shown by [58]. But if oscillating fins are contributing to F_c, then R will decrease to zero as V^2/U^2 decreases to zero (or, effectively, as V decreases to zero). Second, because the velocity components of equation (3) are both squared, R will scale with body length as L^{-1} and the relative performance, R/L, will be a function of V^2/U^2.

Because of the broad range of experimental differences among the studies, including the focal behavior (fast starts, routine turns, feeding turns) and the method of estimating the turning radius, we can draw few conclusions from the variation in minimum R measured among different fishes (Fig. 7). The least squares slope though all data is 1.8, which differs significantly from a slope of one, but this value should be interpreted cautiously. One might expect PF turns to be

sharper than CB turns, since the pair of pectoral fins on each side of the turning axis can generate pure torque (by canceling out each other's translational components). For coral reef fishes that use the pectoral fins to generate turning moments, turning radius is not a function of body stiffness (and, indeed, this relationship would not be expected) [52]. But among the flexible, coral reef fishes, CB turns are sharper than PF turns [4], which is contrary to expectations since the caudal body acting alone has no ability to generate rotational moments without translation. Unfortunately, it is not clear to what extent the CB turns of the coral reef fishes are using the pectoral fins to cancel translational components. Indeed, CB turns among fishes that are less active with their fins during yaw turns (trout, tuna) have higher turning radii.

2) Linear Acceleration. Acceleration is simply a function of the thrust and the resistance to acceleration, $a = T/m$, where T is the circulatory and inertial thrust and m is the virtual mass. At high accelerations, the inertial component should dominate the thrust balance. This inertial component can be modeled by

$$T_i = \tfrac{1}{4}\rho\pi\int c^2 \dot{U}_N \, dR \tag{4}$$

where c is the depth or chord of the control surface, $\dot{U}_N$ is the normal acceleration of the control surface and ρ is an added mass coefficient. Increased depth (but not breadth) in regions of the control surface that have the highest normal accelerations are expected to increase acceleration [59]. Thus we would expect distally-expanding fins in fishes that use fins for accelerating water [60] and caudally positioned and deep median fins in fishes that use the caudal body to generate large accelerations [61]. Normal accelerations can be increased by decreasing non-muscle mass, increasing the proportion of type IIx fibers in the muscles actuating the control surface, or by increasing the mechanical advantage of the musculoskeletal system.

Maximum CB-powered accelerations have been measured for many fishes (Fig. 8) but there are no PF- or CF-powered accelerations for comparison with each other or with CB turns. Kinematic and morphological factors of acceleration performance have been frequently addressed but unambiguous results are uncommon. In general, C-starts produce higher accelerations and are associated with larger turning angles than S-starts [10]. Within C-starts it has been suggested that greater axial curvatures along the body at the end of stage I should produce larger accelerations and there is some evidence to support this [62-64]. In contrast, [65] found a negative association between acceleration performance and maximum curvature. Finally, in a comparison of C-starts among six fishes, [66] found that maximum accelerations were a function of the wave speed of body bending but not of body curvature. Morphological features that have been proposed as augmenting acceleration performance include increased body depth, decreased body depth, increased median and caudal fin area, caudally positioned median fins, increased flexural stiffness, and reduced flexural stiffness. There are no good comparative or experimental data to support any of these hypotheses, with the exception of a fin ablation experiment supporting the hypotheses that increased fin area in the caudal region of the body augments acceleration performance [61].

Because isometric muscle tension is proportional to L^2 and the inertial resistance to acceleration is proportional to L^3, it has been assumed that maximum acceleration scales as $L^2/L^3 = L^{-1}$. But the thrust available for acceleration is less a function of isometric muscle tension than with the output force of the geared musculoskeletal sytem [67]

$$F_{out} = F_{dyn}\frac{d_{in}}{d_{out}} \tag{5}$$

where F_{dyn} is the maximum dynamic muscle tension, and d_{in} and d_{out} are the input and output lever arms, respectively. In contrast to the expectation from isometric muscle tension scaling, Marden and Allen [68] showed that F_{out} scales to L^3 across a broad range of animal and human-engineered motor systems and over a x-fold range in scale. If the available force for acceleration is proportional to L^3 and mass scales isometrically, then maximum acceleration should scale with an exponent of zero. Indeed both among species (Fig. 8) and within species [69, 70], acceleration is independent of size (larval and juvenile fishes are an exception [55, 71]. This change in acceleration within early post-hatching ontogeny probably results from changing kinetic properties of the myotomal muscle). Allometric scaling of F_{dyn}, d_{in}, and d_{out} has not been investigated in fishes. Among dragonflies, maximum dynamic muscle tension scaled with a length exponent of 2.52, which was significantly greater than the expected isometric scaling of 2.0 [67].

3) Rotational Velocity. High rotational-velocity turns are achieved by generating large forces with long moment arms. Circulatory (Drag and Lift) and inertial (acceleration reaction) forces, in turn, are functions of both the area of the control surface and the velocity (circulatory) or change in velocity (inertial) of the incident flow over the control surface. Three lines of evidence suggest that CB turns should be fastest. First, the center of mass of fish lies somewhere in the anterior half of the body, a position that will generally give the caudal body a moment arm nearly as long as the caudal fin by itself and much longer than that of either pectoral fin. Second, peak velocities and normal accelerations of the center of force of the caudal body are higher than for either the pectoral fin or the caudal fin because the longer span of the caudal body and because the muscles powering caudal body deformations are larger and have higher proportions of fast twitch fibers than muscles powering the pectoral or caudal fin rays. Finally, the area of the caudal body is larger than the areas of either the caudal fin or pectoral fins.

Both mean rotational velocities, Ω_{avg}, and peak rotational velocities, Ω_{max}, have been reported. A comparison of measured rotational velocities among PF, CF, and CB powered turns (Fig. 9) supports the prediction that CB turns are fastest. Some of the difference between turning types is due to motivation; the PF data are from routine turns while the CB data are from both routine turns and highly stereotyped, fast-start escape responses, or C-starts, that are used to rapidly move the fish out of the path of a striking predator. Limiting the comparison to routine turns shows that routine CB turns are higher than PF turns (Fig 9). For CB turns, axial bending not only increases the amplitude (and

torque) of the caudal fin but also allows the tail and median fins to contribute to the torque. Because of their stiff, bony carapace that precludes axial bending anterior to the caudal peduncle, boxfishes provide the unusual opportunity to measure rotational velocity in CF turns in which pre-peduncle axial bending cannot augment performance. In the boxfish *Ostracion cubicus*, the caudal fin is only actively oscillated in startle maneuvers. Boxfish CF startle turns are faster than PF turns but are slower than the CB C-starts of more flexible fish (Fig. 9). Again, the faster CF turns relative to PF turns in *O. cubicus* should not be surprising. While fin areas and moment arms have not been measured in *O. cubicus*, [18] showed that the area of the caudal fin is 42% greater than the summed area of both pectoral fins in *O. meleagris*.

While axial bending should decrease both viscous and inertial resistance to rotation, estimates of rotational drag and moments of inertia for different amounts of axial deformation have not been investigated. Pectoral fins that are longer, have more of the area distributed toward the tip (i.e. higher radial moments of area about the fin base), and move with a more rowing-like motion will generate larger turning moments than fins with the opposite phenotypes [23, 60]. This suggests that fishes with fan-shaped, rowing fins can generate higher pectoral-fin powered rotational velocities than can fishes with wing-shaped, flapping fins. This hypothesis has not been formally tested but a comparison of turns between boxfishes, with fan-shaped fins, and species of wrasse, surgeonfish, and angelfish with wing-shaped fins do not support the hypothesis. As with all comparative tests of causal hypotheses, however, the comparison is confounded by unmeasured variables and uncontrolled variation. For example, a boxfish has a larger second moment of mass (moment of inertia) than a wrasse of equal length when at rest, and this difference increases during a turn because of the wrasse's ability to bend.

4) Miscellaneous Yaw Turning Performance. One aspect of maneuverability is the ability to easily move within confined spaces. Based on qualitative comparisons of fishes among habitats, functional ichthyologists have generally concluded that a combination of a deep body and laterally positioned pectoral fins facilitates maneuverability and the exploitation of resources in structurally rich habitats such as aquatic vegetation and coral reefs [72, 73]. Variation in the ability to maneuver in confined spaces was compared among goldfish (*Carassius auratus*), silver dollar (*Metynnis hypsaurchen*), and angelfish (*Pterophyllum scalare*) by coercing these fishes to negotiate slits and tubes of various geometries [74-76] (it should be noted that the ability to move in an enclosed space is not the same as the ability to exploit resources in structurally complex habitats and the optimum body shapes in these habitats may radically differ. Compare the eel-shaped design of the crevice denizens with the pancake-shaped design of the fishes maneuvering among coral, but not within it). Relative to goldfish, silver dollars and angelfish, with their deep and narrow bodies, were able to move though 63% and 45% narrower tubes per cube-root unit body mass, respectively (note that my interpretation of the data, which is based on standardizing by body mass, is consistent with that of [74] but differs from that of [75], which is based on standardizing by total length. I am explicitly asking the question, "given a fish with a certain unit mass, what is the best distribution of the mass itself and of fins around the mass to facilitate maneuvering through slits and tubes?"). In contrast, goldfish can turn in smaller bent tubes and the goldfish performance, relative to that of silver dollars and angelfish, increases with the magnitude of the bend [76]. While these confinement experiments ultimately failed to discover the general principles of optimal body and fin design for open water maneuverability, they did show that expected optimal designs for open water maneuvering are relatively poor designs for maneuvering in confined spaces (see also [52]).

IV. Conclusion and Future Work.

The repeated associations between diverse morphologies and habitats among fishes enabled the development of a general theory of body and fin function in fish [72, 73]. Two decades of swimming research on fishes, however, have demonstrated the difficulty of extracting the causal anatomical and kinematic features that augment maneuverability. For yaw turns, available comparative data show that

- stiff bodied fishes can turn with minimum turning radii if the turning moments are generated by oscillating pectoral fins [52].
- for caudal body powered turns, more flexible fish have smaller turning radii [10].
- powering a turn with the caudal fin alone or the caudal body with stiff, erect median fins generates faster rotations than powering a turn with the pectoral fins (Fig. 9).
- increasing posterior fin area increases acceleration performance [61].

These are all very general conclusions. We have too few data to draw any inference about how variation in control surface (including the fins and body) shape and motion causally affect maneuvering performance. We have few data on behaviors other than yaw turns (indeed other than fast start yaw turns), including hovering, braking, and pitching. It has been two decades since the introduction of Webb's seminal model of fish locomotor morphology [72, 73], but we still have no empirical data confirming mechanical models of many of the major, conspicuous patterns in fish diversity, such as the repeated association between structurally complex habitats and fishes with short, narrow, and deep bodies and dorsally positioned pectoral fins.

To rectify this deficiency, live animal research should focus on four areas. First, we need more detailed information on the biotic and abiotic features of environments that stimulate maneuvering behavior and how fishes respond to these stimuli. Replication of the stimuli in the lab would allow more controlled measurements of maneuvering performance. Related to this is, what are the important measures of maneuverability for comparison? Broad differences in turning radius appear associated with broad behavioral differences; pelagic or migratory fishes with less active pectoral fins and relatively stiff bodies have higher turning radii than coral reef fishes with active pectoral fins and/or flexible bodies. But are small (if at all) differences in turning radius part of the explanation for body shape

variation among coral reef fishes? Other than fast starts (for which it is probably less relevant), there are no studies measuring the energy required to turn or to stabilize perturbations to the heading. Keels on the body of the boxfish, *Lactophrys triqueter*, act as passive control surfaces that self-correct perturbations to the heading during steady swimming [77]. Perhaps the focus on highly maneuverable fishes should focus more on energetic consequences of variation in control surface shape and movement.

Second, we need more detailed anatomical and kinematic descriptions. Important anatomical measures include: fin mass, moments of fin area and mass, body mass, and moments of body and fin area and mass about each rotational axis. Kinematic descriptions that follow those for flapping insect wings (e.g. [33]) are not sufficient for maneuvering because of the greater complexity of fin deformations. In addition to the typically reported frequency and amplitude of the leading edge ray, stroke plane angle, and geometric angles of attack, we need better quantitative measures of fin deformations than the qualitative descriptions given for the stickleback and boxfish above. Importantly, we need these anatomical and kinematic descriptions in combination with performance measures. The former are typically collected by biomechanical physiologists less interested in performance and more interested in developing models of how deforming fins and bodies generate fluid dynamic forces. Performances are typically measured by ecologists who largely treat the functional morphology as a black box.

Finally we need more studies that control confounding variables either statistically, or, preferably, experimentally. Comprehensive, phylogenetically controlled comparisons among many closely related species offers the best comparative method for inferring causal relationships between morphology and performance. Additional causal variables are controlled statistically (if measured) or by careful sampling. Uncontrolled variation is, hopefully, distributed in a way that does not confound the results. Phenotypic manipulation studies offer the possibility of controlling causal and confounding variables experimentally. The less-than-satisfactory control of variation in comparative studies and difficulty of designing phenotypic manipulation experiments suggests that simulation experiments using computational and physical modeling will prove valuable in future work on the performance consequences of phenotypic variation [41].

REFERENCES

[1] P. J. Geerlink, "The role of the pectoral fins in braking of mackerel, cod and saithe," *Netherlands Journal of Zoology*, vol. 37, pp. 81-104, 1987.

[2] J. J. Videler, *Fish Swimming*. London: Chapman & Hall, 1993.

[3] K. D'Août and P. Aerts, "A kinematic comparison of forward and backward swimming the eel *Anguilla anguilla*," *Journal of Experimental Biology*, vol. 202, pp. 1511-1521, 1999.

[4] C. L. Gerstner, "Maneuverability of four species of coral-reef fish that differ in body and pectoral-fin morphology," *Canadian Journal of Zoology*, vol. 77, pp. 1102-1110, 1999.

[5] P. W. Webb and A. G. Fairchild, "Performance and maneuverability of three species of teleostean fishes," *Canadian Journal of Zoology*, vol. 79, pp. 1866-1877, 2001.

[6] G. V. Lauder, "Caudal fin locomotion in ray-finned fishes: historical and functional analyses," *Amer. Zool.*, vol. 29, pp. 85-102, 1989.

[7] D. Weihs, "A hydrodynamical analysis of fish turning manoeuvres," *Proceedings of the Royal Society of London, B*, vol. 182, pp. 59-72, 1972.

[8] P. Domenici and R. S. Batty, "Escape behavior of solitary herring (*Clupea harengus*) and comparisons with schooling individuals," *Marine Biology*, vol. 128, pp. 29-38, 1997.

[9] S. A. Budick and D. M. O'Malley, "Locomotor repetoire of the larval zebrafish: swimming, turning and prey capture," *Journal of Experimental Biology*, vol. 203, pp. 2565-2579, 2000.

[10] P. Domenici and R. W. Blake, "The kinematics and performance of fish fast-start swimming," *Journal of Experimental Biology*, vol. 200, pp. 1165-1178, 1997.

[11] T. L. Daniel, "Forward flapping flight from flexible fins," *Canadian Journal of Zoology*, vol. 66, pp. 630-638, 1988.

[12] S. A. Combes and T. L. Daniel, "Shape, flapping and flexion: wing and fin design for forward flight," *Journal of Experimental Biology*, vol. 204, pp. 2073-2085, 2001.

[13] L. J. Rosenberger, "Pectoral fin locomotion in batoid fishes: Undulation versus oscillation," *Journal of Experimental Biology*, vol. 204, pp. 379-394, 2001.

[14] B. Wright, "Form and function in aquatic flapping propulsion: Morphology, kinematics, hydrodynamics, and performance of the triggerfishes (Tetraodontiformes: Balistidae)," in

Organismal Biology and Anatomy. Chicago: University of Chicago, 2000, pp. 316.

[15] E. G. Drucker and G. V. Lauder, "Locomotor function of the dorsal fin in teleost fishes: experimental analysis of wake forces in sunfish," *Journal of experimental Biology*, vol. 204, pp. 2943-2958, 2001.

[16] M. S. Gordon, I. Plaut, and D. Kim, "How puffers (Telostei: Tetraodontidae) swim," *Journal of Fish Biology*, vol. 49, pp. 319-328, 1996.

[17] V. I. Arreolla and M. W. Westneat, "Mechanics of propulsion by multiple fins: Kinematics of aquatic locomotion in the burrfish (*Chilomycterus schoepfi*)," *Proceedings of the Royal Society of London, B*, vol. 263, pp. 1689-1696, 1996.

[18] J. R. Hove, L. M. O'Bryan, M. S. Gordon, P. W. Webb, and D. Weihs, "Boxfishes (Teleostei: Ostraciidae) as a model system for fishes swimming with many fins: kinematics," *Journal of Experimental Biology*, vol. 204, pp. 1459-1471, 2001.

[19] R. W. Blake, "On ostraciiform locomotion," *Journal of the Marine Biological Association of the United Kingdom*, vol. 57, pp. 1047-1055, 1977.

[20] C. M. Breder, Jr., "The locomotion of fishes," *Zoologica*, vol. 4, pp. 159-291, 1926.

[21] R. W. Blake, "Median and paired fin propulsion," in *Fish Biomechanics*, P. W. Webb and D. Weihs, Eds. New York: Praeger, 1983, pp. 214-247.

[22] S. Vogel, *Life in Moving Fluids (2nd Ed.)*, 2nd ed. Princeton: Princeton University Press, 1994.

[23] J. A. Walker and M. W. Westneat, "Mechanical performance of aquatic rowing and flying," *Proceedings of the Royal Society of London, B*, vol. 267, pp. 1875-1881, 2000.

[24] J. A. Walker and M. W. Westneat, "Kinematics, dynamics, and energetics of rowing and flapping propulsion," *Integrative and Comparative Biology*, 2002.

[25] C. J. Fulton, D. R. Bellwood, and P. C. Wainwright, "The relationship between swimming ability and habitat use in wrasses (Labridae)," *Marine Biology*, vol. 139, pp. 25-33, 2001.

[26] D. R. Bellwood and P. C. Wainwright, "Locomotion in labrid fishes: implications for habitat use and cross-shelf biogeography on the Great Barrier Reef," *Coral Reefs*, vol. 20, pp. 139-150, 2001.

[27] P. C. Wainwright, D. R. Bellwood, and M. W. Westneat, "Ecomorphology of locomotion in labrid fishes," *Environmental Biology of Fishes*, vol. 65, pp. 47-62, 2002.

[28] P. J. Geerlink, "The anatomy of the pectoral fin in Sarotherodon niloticus trewavas (Cichlidae)," *Netherlands Journal of Zoology*, vol. 29, pp. 9-32, 1979.

[29] P. W. Webb, "Kinematics of pectoral fin propulsion in *Cymatogaster aggregata*," *Journal of Experimental Biology*, vol. 59, pp. 697-710, 1973.

[30] P. J. Geerlink, "Pectoral fin kinematics of *Coris formosa* (Teleostei, Labridae)," *Netherlands Journal of Zoology*, vol. 33, pp. 515-531, 1983.

[31] A. Gibb, B. C. Jayne, and G. V. Lauder, "Kinematics of pectoral fin locomotion in the bluegill sunfish *Lepomis macrochirus*," *Journal of Experimental Biology*, vol. 189, pp. 133-161, 1994.

[32] G. V. Lauder and B. C. Jayne, "Pectoral fin locomotion in fishes: testing drag-based models using three-dimensional kinematics," *American Zoologist*, vol. 36, pp. 567-581, 1996.

[33] J. A. Walker and M. W. Westneat, "Labriform propulsion in fishes: Kinematics of flapping aquatic flight in the bird wrasse *Gomphosus varius* (Labridae)," *Journal of Experimental Biology*, vol. 200, pp. 1549-1569, 1997.

[34] J. A. Walker and M. W. Westneat, "Performance limits of labriform propulsion and correlates with fin shape and motion," *Journal of Experimental Biology*, vol. 205, pp. 177-187, 2002.

[35] E. G. Drucker and G. V. Lauder, "Function of pectoral fins in rainbow trout: behavioral repertoire and hydrodynamic forces,"

Journal of Experimental Biology, vol. 206, pp. 813-826, 2003.

[36] M. H. Dickinson, F.-O. Lehmann, and S. P. Sane, "Wing rotation and the aerodynamic basis of insect flight," *Science*, vol. 284, pp. 1954-1960, 1999.

[37] N. Kato and H. Liu, "Load characteristics of a three-motor-driven mechanical pectoral fin," *Journal of Fluids Engineering*, 2003.

[38] N. Kato, "Hydrodynamic characteristics of mechanical pectoral fin," *Journal of Fluids Engineering*, vol. 121, pp. 605-613, 1999.

[39] P. J. Geerlink, "Pectoral fin morphology: a simple relation with movement pattern?," *Netherlands Journal of Zoology*, vol. 39, pp. 166-193, 1989.

[40] D. Adriaens, D. Decleyre, and W. Verraes, "Morphology of the pectoral girdle in Pomatoschistus lozanoi de Buen, 1923 (Gobiidae), in relation to pectoral fin adduction," *Belgian Journal of Zoology*, vol. 123, pp. 135-157, 1993.

[41] J. A. Walker, "Functional morphology and virtual models: Physical constraints on the design of oscillating wings, fins, legs, and feet at intermediate Reynolds numbers," *Integrative and Comparative Biology*, vol. 42, pp. 232-242, 2002.

[42] M. H. Dickinson, F. O. Lehmann, and K. G. Götz, "The active control of wing rotation by *Drosophila*," *Journal of Experimental Biology*, vol. 182, pp. 173-189, 1993.

[43] F. E. Fish, R. V. Baudinette, P. B. Frappell, and M. P. Sarre, "Energetics of swimming by the platypus *Ornithorhynchus anatinus*: Metabolic effort associated with rowing," *Journal of Experimental Biology*, vol. 200, pp. 2647-2652, 1997.

[44] C. M. Pace, R. W. Blob, and M. W. Westneat, "Comparative kinematics of the forelimb during swimming in red-eared slider (*Trachemys scripta*) and spiny softshell (*Apalone spinifera*) turtles," *Journal of Experimental Biology*, vol. 204, pp. 3261-3271, 2001.

[45] G. Hughes, "The co-ordination of insect movements. 3. Swimming in Dytiscus, Hyrophilus, and a dragonfly nymph," *Journal of Experimental Biology*, vol. 35, pp. 567-583, 1958.

[46] W. Nachtigall, "Locomotion: Mechanics and hydrodynamics of swimming in aquatic insects," in *The Physiology of insecta*, vol. III, M. Rockstein, Ed. New York: Academic Press, 1974, pp. 381-432.

[47] S. Sane and M. H. Dickinson, "The control of flight force by a flapping wing: lift and drag production," *journal of experimental Biology*, vol. 204, pp. 2607-2626, 2001.

[48] J. A. Walker, "Rotational lift: Something different or more of the same?," *Journal of Experimental Biology*, vol. 205, pp. 3783-3792, 2002.

[49] T. A. Williams, "A model of rowing propulsion and the ontogeny of locomotion in *Artemia* larvae," *Biological Bulletin*, vol. 187, pp. 164-173, 1994.

[50] M. A. R. Koehl, "Hairy little legs: feeding, smelling, and swimming at low Reynolds numbers," *Contemporary Mathematics*, vol. 141, pp. 33-47, 1993.

[51] R. W. Blake, "The swimming of the mandarin fish *Synchropus picturatus* (Callionyiidae: Teleostei)," *Journal of the Marine Biological Association of the United Kingdom*, vol. 59, pp. 421-428, 1979.

[52] J. A. Walker, "Does a rigid body limit maneuverability?," *Journal of Experimental Biology*, vol. 203, pp. 3391-3396, 2000.

[53] E. G. Drucker and G. V. Lauder, "Wake dynamics and fluid forces of turning maneuvers in sunfish," *Journal of Experimental Biology*, vol. 204, pp. 431-442, 2001.

[54] P. R. Bandyopadhay, J. M. Castano, J. Q. Rice, B. Philips, W. H. Nedderman, and W. K. Macy, "Low-speed maneuvering hydrodynamics of fish and small underwater vehicles," *Journal of Fluids Engineering*, vol. 119, pp. 136-144, 1997.

[55] J. M. Wakeling, K. M. Kemp, and I. A. Johnston, "The biomechanics of fast-starts during ontogeny in the common carp *Cyprinus carpio*," *Journal of Experimental Biology*, vol. 202, pp. 3057-3067, 1999.

[56] P. Domenici, "Scaling the locomotor performance of aquatic vertebrates during predator-prey interactions: from fish to killer whales," *Comparative Biochemistry*

and Physiology, vol. 131, pp. 169-182, 2001.

[57] P. Domenici and R. W. Blake, "The kinematics and performance of the escape response in the angelfish (*Pterophyllum eimekei*)," *Journal of Experimental Biology*, vol. 156, pp. 187-205, 1991.

[58] P. W. Webb, "Speed, acceleration and manoeuverability of two teleost fishes," *Journal of Experimental Biology*, vol. 102, pp. 115-122, 1983.

[59] D. Weihs, "Design features and mechanics of axial locomotion in fish," *American Zoologist*, vol. 29, pp. 151-160, 1989.

[60] R. W. Blake, "Influence of pectoral fin shape on thrust and drag in labriform locomotion," *Journal of Zoology*, vol. 194, pp. 53-66, 1981.

[61] P. W. Webb, "Effects of median-fin amputation on fast-start performance of rainbow trout (*Salmo gairdneri*)," *Journal of Experimental Biology*, vol. 68, pp. 123-135, 1977.

[62] E. B. Taylor and J. D. McPhail, "Prolonged and burst swimming in anadromous and freshwater threespine stickleback, *Gasterosteus aculeatus*," *Canadian Journal of Zoology*, vol. 64, pp. 416-420, 1986.

[63] G. M. Andraso and J. N. Barron, "Evidence for a trade-off between defensive morphology and startle-response performance in the brook stickleback (*Culaea inconstans*)," *Canadian Journal of Zoology*, vol. 73, pp. 1147-1153, 1995.

[64] G. M. Andraso, "A comparison of startle response in two morphs of the brook stickleback (*Culaea inconstans*): further evidence for a trade-off between defensive morphology and swimming ability," *Evolutionary Ecology*, vol. 11, pp. 83-90, 1997.

[65] M. W. Westneat, M. E. Hale, M. J. McHenry, and J. H. Long, Jr., "Mechanics of the fast-start: muscle function and the role of intramuscular pressure in the escape behavior of *Amia calva* and *Polypterus palmas*," *Journal of Experimental Biology*, vol. 201, pp. 3041-3055, 1998.

[66] J. M. Wakeling and I. A. Johnston, "Muscle power output limits fast-start performance in fish," *Journal of Experimental Biology*, vol. 201, pp. 1505-1526, 1998.

[67] R. J. Schilder and J. H. Marden, "A hierarchical analysis of the scaling of force production by dragonfly flight motors," *Journal of Experimental Biology*, 2003.

[68] J. H. Marden and L. R. Allen, "Molecules, muscles, and machines: Universal performance characteristics of motors," *Proceedings of the National Academy of Sciences, USA*, vol. 99, pp. 4161-4166, 2002.

[69] P. W. Webb, "The effect of size on the fast-start performance of rainbow trout, *Salmo gairdneri*, and a consideration of piscivorous predator-prey interactions," *Journal of Experimental Biology*, vol. 65, pp. 157-177, 1976.

[70] P. Domenici and R. W. Blake, "The effect of size on the kinematics and performance of angelfish (*Pterophyllum eimekei*) escape responses," *Canadian Journal of Zoology*, vol. 71, pp. 2319-2326, 1993.

[71] M. E. Hale, "Locomotor mechanics in early life history: effects of size and ontogeny on fast-start performance in salmonid fishes," *Journal of Experimental Biology*, vol. 202, pp. 1465-1479, 1999.

[72] P. W. Webb, "Locomotor patterns in the evolution of actinopterygian fishes," *American Zoologist*, vol. 22, pp. 329-342, 1982.

[73] P. W. Webb, "Body form, locomotion and foraging in aquatic vertebrates," *American Zoologist*, vol. 24, pp. 107-120, 1984.

[74] P. W. Webb, G. D. LaLiberte, and A. J. Schrank, "Do body and fin form affect the maneuverability of fish traversing vertical and horizontal slits?," *Environmental Biology of Fishes*, vol. 46, pp. 7-14, 1996.

[75] A. J. Schrank and P. W. Webb, "Do body and fin form affect the abilities of fish to stabilize swimming during maneuvers through vertical and horizontal tubes?," *Environmental Biology of Fishes*, vol. 53, pp. 365-371, 1998.

[76] A. J. Schrank, P. W. Webb, and S. Mayberry, "How do body and paired-fin positions affect the ability of three teleost fishes to maneuver around bends?,"

Canadian Journal of Zoology, vol. 77, pp. 203-210, 1999.

[77] I. K. Bartol, M. Gharib, D. Weihs, P. W. Webb, J. R. Hove, and M. Gordon, "Hydrodynamic stability of swimming in ostraciid fishes: role of the carapace in the smooth trunkfish *Lactophys triqueter* (Teleostei: Ostraciidae)," *Journal of Experimental Biology*, vol. 206, pp. 725-744, 2003.

[78] G. K. Temple and I. A. Johnston, "Testing hypotheses concerning the phenotypic plasticity of escape performance in fish of the family Cottidae," *Journal of Experimental Biology*, vol. 201, pp. 317-331, 1998.

[79] T. C. Law and R. W. Blake, "Comparison of fast-start performances of closely related, morphologically distinct threespine sticklebacks (*Gasterosteus* spp.)," *Journal of Experimental Biology*, vol. 199, pp. 2595-2604, 1996.

[80] A. K. Gamperl, D. L. Schnurr, and E. D. Stevens, "Effect of sprint-training protocol on acceleration performance in rainbow trout (Salmo gairdneri)," *Canadian Journal of Zoology*, vol. 69, pp. 578-582, 1991.

[81] D. G. Harper and R. W. Blake, "Fast-start performance of rainbow trout *Salmo gairdneri* and northern pike *Esox lucius*," *Journal of Experimental Biology*, vol. 150, pp. 321-342, 1990.

[82] M. A. Kasapi, P. Domenici, R. W. Blake, and D. Harper, "The kinematics and performance of escape responses of the knifefish *Xenomystus nigri*," *Canadian Journal of Zoology*, vol. 71, pp. 189-195, 1993.

[83] I. L. Y. Spierts and J. L. van Leeuwen, "Kinematics and muscle dynamics of C- and S-starts of carp (*Cyprinus carpio* L.)." *Journal of Experimental Biology*, vol. 202, pp. 393-406, 1999.

[84] E. Tytell and G. V. Lauder, "The C-start escape response of *Polypterus senegalus*: bilateral muscle activity and variation during stage 1 and 2," *Journal of Experimental Biology*, vol. 205, pp. 2591-2603, 2002.

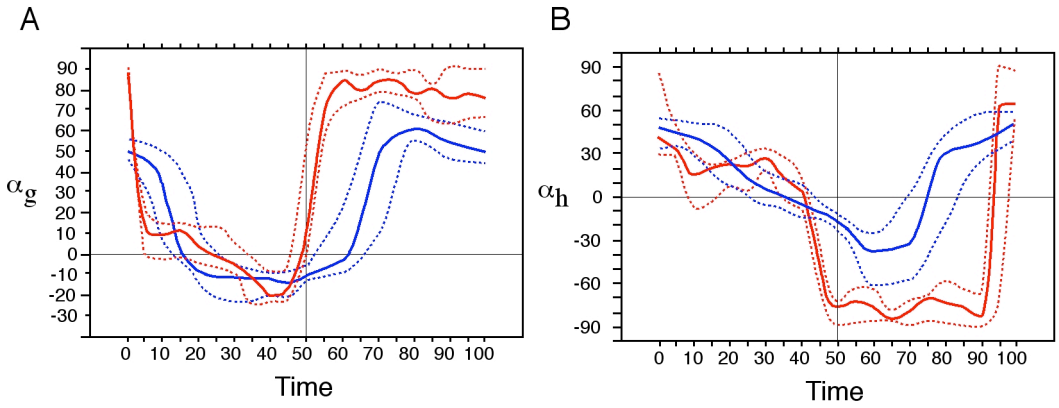

Fig. 1. Geometric (A) and hydrodynamic (B) angles of attack for the rowing stroke of the threespine stickleback (red), *Gasterosteus aculeatus*, and the flapping stroke of the bird wrasse (blue), *Gomphosus varius*. The solid lines represent the mean attack angles while the dashed lines represent the 90% confidence intervals. Modified from [24].

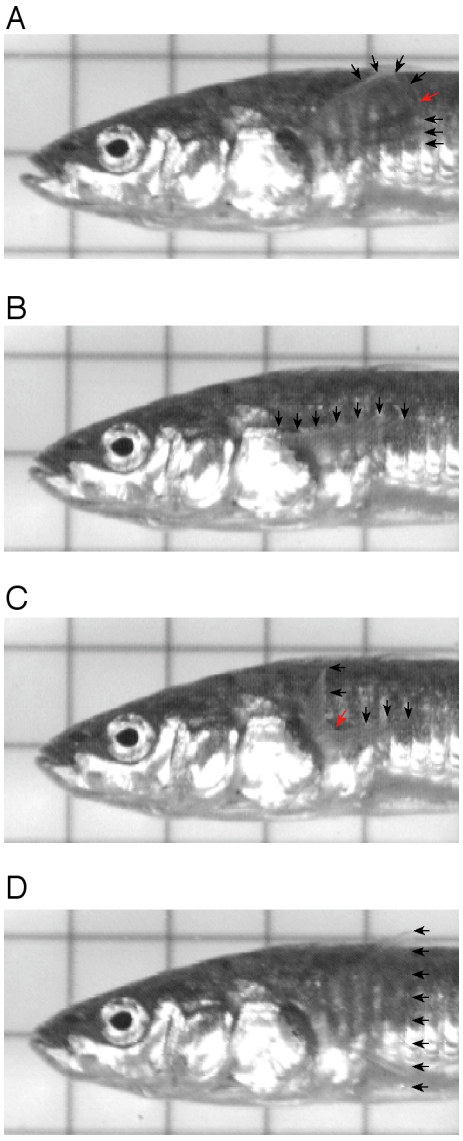

Fig. 2. The rowing stroke of the threespine stickleback during steady swimming. (A) Fin rays, beginning with the leading edge, are sequentially "peeling" off the body during the first part of abduction. (B) Feathered orientation during the last part of abduction. (C) Beginning of adduction. As the leading edge actively adducts, inactive posterior rays sequentially activate and adduct with the leading edge. (D) End of adduction as the fin closes against the body.

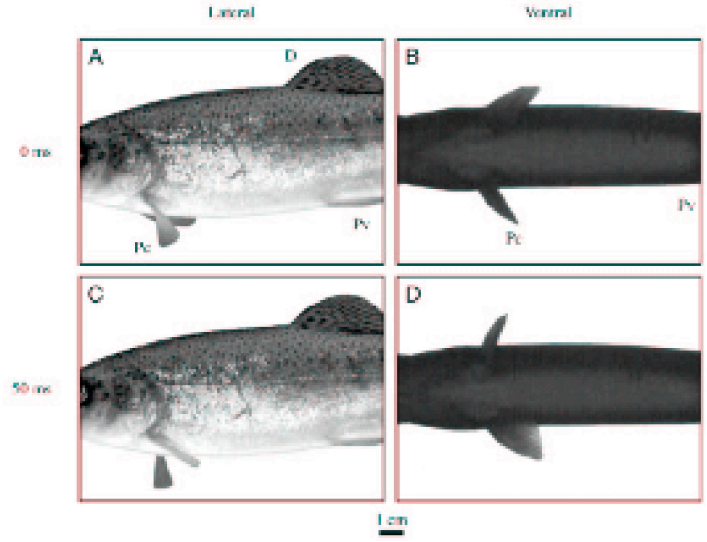

Fig. 3. "paddling" hovering stroke of the rainbow trout, *Oncorhychus mykiss*. From [35].

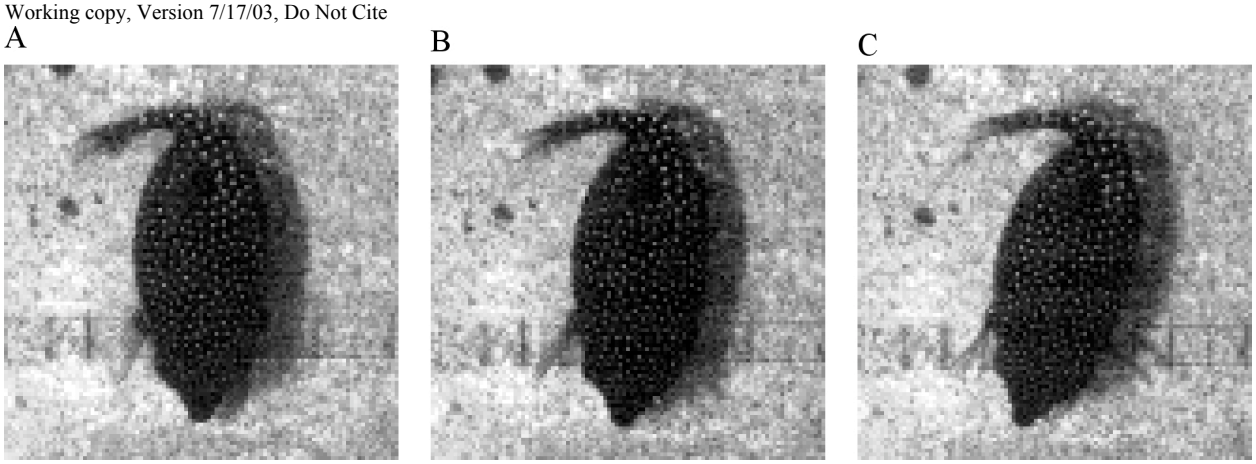

Fig. 4. The power stroke of the inside fin during a turn in the boxfish, *Ostracion meleagris*. In (A) the fin is in a feathered orientation with the leading edge ray maximally abducted of all rays (note that in some fin strokes during turns, the fin can be feathered opposite to that shown here, that is, with the leading edge minimally abducted and the trailing edge ray maximally abducted). In (B), the fin has rotated (supinated) about the leading edge causing the trailing edge to abduct and the fin to enter a broadside orientation. In (C), the trailing edge ray has continued to abduct to a position greater than 180° so that it is now more abducted than the leading edge ray.

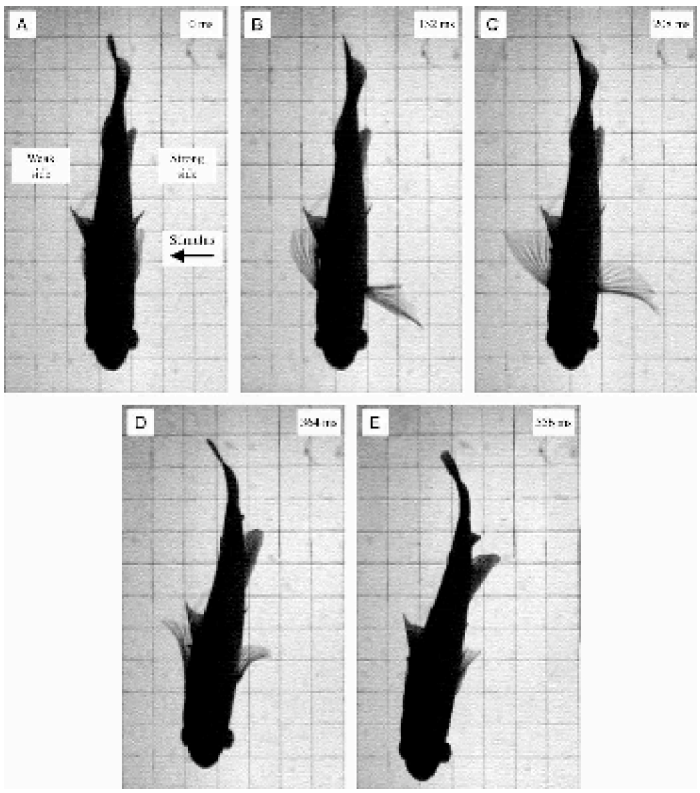

Fig. 5. Pectoral and dorsal fin motion during a small yaw turn in a bluegill sunfish, *Lepomis macrochirus*, swimming in a slow flow (0.5 L/s). From [53].

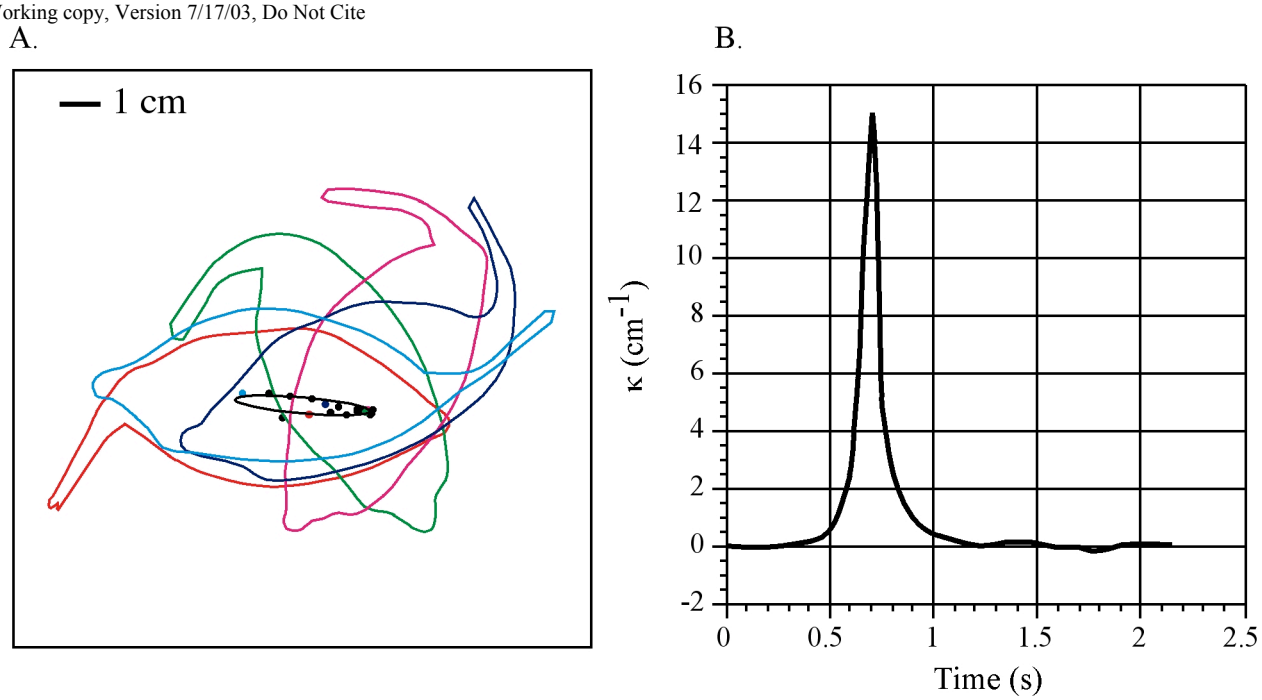

Fig. 6. Turning of the boxfish, *Ostracion meleagris*. (A) outlines of the body and the corresponding path of the center of math illustrate that body rotation occurs both prior to and following the change in direction of the center of mass. The magnitude of the major and minor axes of the scatter of points along the turning path (represented by the ellipse) are parameters describing the turning performance. (B) the change in the curvature (□), which is the reciprocal of the radius of curvature, along the turning path illustrated in (A). The curvature is low for most of the turn but has a sharp peak where the center of mass sharply reversed direction.

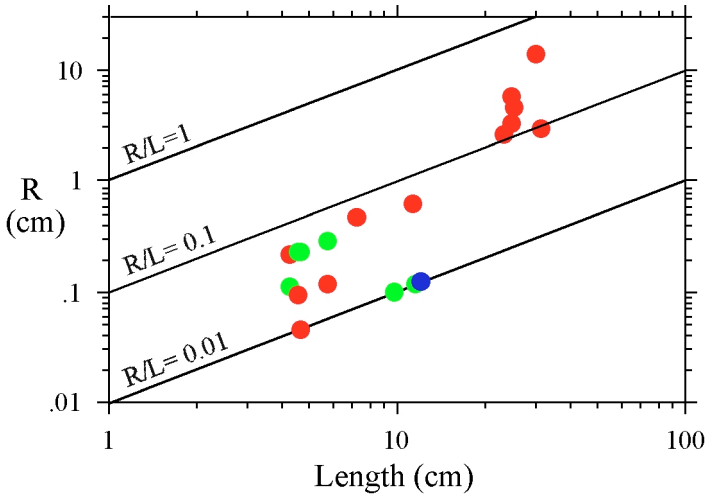

Fig. 7. Minimum turning radius measured for different fishes from caudal body turns (red), pectoral fin turns (green), and the caudal fin turn of the boxfish, *Ostracion cubicus*, (blue). Caudal body turns include both routine turns and fast starts. Data from [4, 10, 52] and unpublished data on *O. cubicus*.

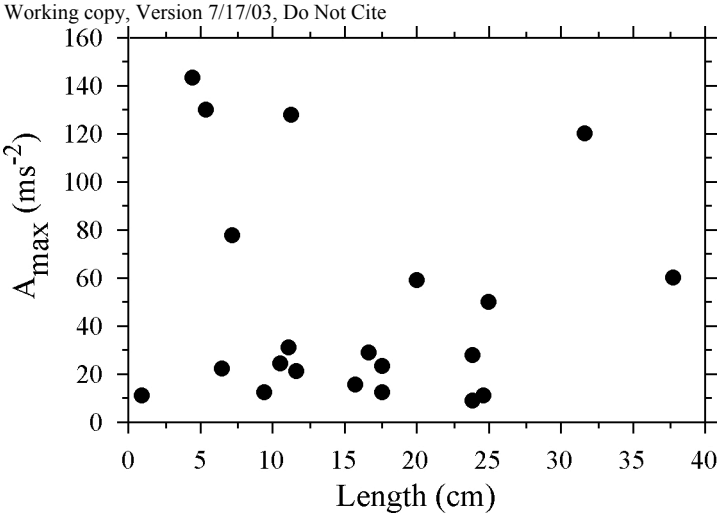

Fig. 8. Species –mean maximum acceleration during fast starts for different fishes as a function of body length. Data from [55, 57, 65, 66, 78-84].

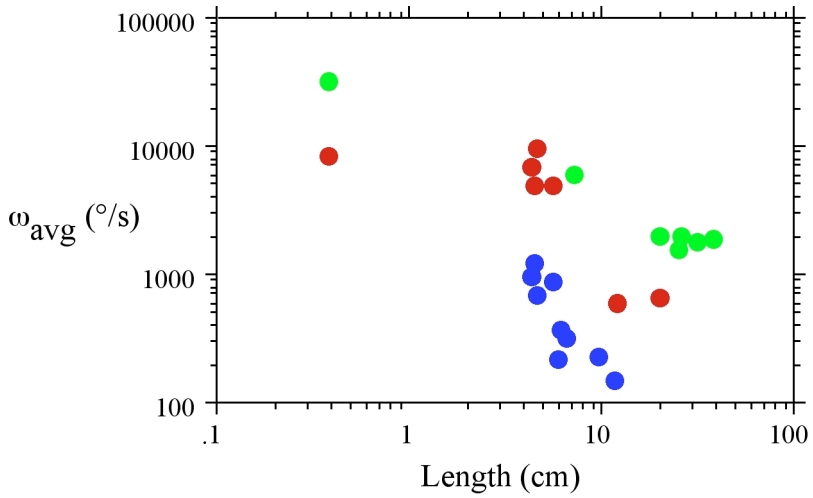

Fig. 9. Maximum average rotational velocities for different fishes during fast starts (green), routine caudal body turns (red) and routine pectoral fin turns (blue). Data from [4, 8, 9, 52, 57, 69, 81, 83] and unpublished data from *Ostracion cubicus*.